Pamukkale Üniversitesi Mühendislik Bilimleri Dergisi
Pamukkale University Journal of Engineering Sciences

Effect of external load on osmotic compression in clay soils

Kil zeminlerde harici yükün ozmotik sikişmaya etkisi

Uğur Eren Yurtcan[1], Selim Altun[2]*

[1]Construction Department, Vocational School of Technical Sciences, Bingol University, Bingol, Türkiye
ugurereny@gmail.com
[2]Department of Civil Engineering, Faculty of Engineering, Ege University, Izmir, Türkiye
selim.altun@ege.edu.tr

Received/Geliş Tarihi: 18.07.2024 Revision/Düzeltme Tarihi: 03.07.2025 doi: 10.5505/pajes.2025.22379
Accepted/Kabul Tarihi: 19.08.2025 Research Article/Araştırma Makalesi

Abstract

Clay soils that have not been exposed to saltwater can come into contact with brine due to saltwater flooding, sewage intrusion, or similar events. Additional settlements can occur in clays that subsequently interact with brine, driven by the osmotic effect. To investigate this, a series of odometer experiments were conducted on two natural clay samples: one with low plasticity (CL) and one with high plasticity (CH). The low-plasticity samples predominantly contained minerals from the kaolin group, while the high-plasticity samples were rich in minerals from the smectite group. The samples, prepared with distilled water, were exposed to brine solutions of varying concentrations (0.1M, 0.25M, 1M, and 2M NaCl and $CaCl_2$) under specific consolidation pressures (12.5 kPa, 50 kPa, and 200 kPa), simulating osmotically compressed soils. Structural and fabric alterations were examined using SEM images and EDX data collected from the tested samples. It was observed that mechanical forces were the primary factor in the compression of low-plasticity clay, which exhibited minimal fabric changes under the influence of salt. Consequently, osmotic-induced compression and fabric alterations were negligible. For the high-plasticity samples (with high smectite content), the highest osmotic compression was recorded at 50 kPa. These findings highlight the importance of balancing structural stress caused by external loads with osmotic forces.

Anahtar kelimeler: Clay–chemical interaction, time-dependent deformation, osmotic compression, physicochemical effect, SEM, microstructure

Öz

Kil türü zeminler, tuzlu su taşkınları, kanalizasyon sızıntısı vb. nedeniyle tuzlu su ile temas edebilir. Daha sonra tuzlu su ile etkileşime giren killerde ozmotik etkiyle ilave oturmalar meydana gelebilir. Bu amaçla biri düşük plastisiteli (CL) ve diğeri yüksek plastisiteli (CH) olmak üzere iki doğal kil numunesi üzerinde bir dizi ödometre deneyi yapıldı. Düşük plastisiteli numuneler yüksek kaolin grubu mineral içeriğine sahipken, yüksek plastisiteli numuneler yüksek smektit grubu mineral içeriğine sahiptir. Saf su ile hazırlanan ve belirli konsolidasyon basınçlarına kadar (12.5kPa, 50kPa ve 200kPa) yüklenen numuneler tuzlu su çözeltilerine (0.1M, 0.25M, 1M ve 2M NaCl ve $CaCl_2$ çözeltileri) maruz bırakılmış ve yük altında ozmotik sıkışma davranışları incelenmiştir. Deneyler tamamlanan numunelerden elde edilen SEM görüntüleri ve EDX verileri kullanılarak yapısal ve dokusal değişiklikler incelenmeye çalışılmıştır. Dokusu tuzun etkisiyle değişikliğe uğramayan düşük plastisiteli kilin sıkıştırılmasında mekanik kuvvetlerin baskın olduğu gözlemlenmiştir. Bu nedenle ozmotik kaynaklı sıkışma ve doku değişiklikleri ihmal edilebilecek seviyelerde gözlenmiştir. Yüksek plastisiteli numunede (yüksek smektit içeriği) en yüksek ozmotik sıkışmanın 50 kPa'da meydana geldiği gözlenmiştir. Bu nedenle dış yüklerin ve ozmotik kuvvetlerin neden olduğu yapısal yük dengesinin önemli olduğunu ortaya konmuştur.

Keywords: Kil-kimyasal etkileşimi, zamana bağlı deformasyon, osmotik sıkışma, fizikokimyasal etki, SEM, mikro-yapı.

1 Introduction

Tsunamis have posed a threat to coastal settlements throughout history, and today, our coasts remain vulnerable to this natural hazard [1], [2], [3], [4], [5], [6]. As a natural consequence of tsunamis, seawater flooding occurs, leading to an expected increase in the salinity of soil pore water in affected areas. The Mediterranean Sea, one of the saltiest seas in the world, has an average salinity (NaCl) of approximately 3.5% (~0.6M) [7].

Seafloor clays are formed in a saturated state with pore water containing a significantly higher salt concentration. Similarly, marine clays are still forming above sea level today under comparable conditions. To study the properties of these clays, it is essential to use highly concentrated saline solutions[8].

The interaction between clay minerals and pore water of varying chemical composition significantly affects their physical behavior [9], [10], [11], [12], [13], [14], [15], [16]. For example, the performance of clay liners in landfills may deteriorate when exposed to chemical waste [10], [17], [18], [19], [20]. Similarly, chemical leakage beneath industrial foundations can trigger uncontrolled settlements [21], [22]. High NaCl concentrations in clayey slopes may also alter slope stability [23], [24]. These interactions affect key geotechnical parameters such as hydraulic conductivity, swelling, water retention, shear strength, and compressibility [10], [12], [13], [15], [17].

Much of the research on the chemical interactions of clays focuses on soils that have already been exposed to chemical contaminants. In practice, however, such interactions often occur in events like wastewater leakage or seawater flooding. These scenarios involve a gradual process for the clay to fully interact with the contaminant, making it time-consuming. During this interaction, osmotic compression is expected to occur.

Osmotic compression has been widely studied, particularly regarding the interparticle force balance in clays [15], [25], [26], [27], [28], [29], [30], [31]. In addition to chemical effects, clays are also influenced by external loads such as geostatic and structural pressures. Therefore, analyzing settlements requires consideration of both osmotic and mechanical influences.

*Corresponding author/Yazışılan Yazar

To investigate the role of osmotic compression under mechanical loading, two natural clays with contrasting plasticity—CL (low-plasticity, kaolinite-rich) and CH (high-plasticity, smectite-rich)—were subjected to varying levels of effective stress. The samples were exposed to saline solutions containing either monovalent (Na^+) or divalent (Ca^{2+}) cations to evaluate how plasticity, salt concentration, and cation valence affect additional deformation. The experimental program included oedometer tests to assess settlement behavior and SEM-EDX analyses to observe microstructural and chemical changes, providing a comprehensive understanding of the coupled effects of mechanical and osmotic compression.

Di Maio [26] showed that the liquid limit decreases sharply up to 1 M electrolyte concentration, then levels off. Accordingly, salinity levels used in this study (pure water, 0.1 M, 0.25 M, 1 M, and 2 M) reflect this trend. NaCl solutions represent monovalent interactions, while $CaCl_2$ is used to assess valence effects.

Water adsorption significantly influences the mechanical properties of clays [29], [32], [33], [34], [35], [36], [37], [38], [39]. For this reason, this study uses CL (low plasticity, kaolinite-rich) and CH (high plasticity, smectite-rich) clays to represent two distinct water retention behaviors (Table 1).

To simulate soil behavior under saltwater intrusion, samples initially prepared with pure water were loaded to a specific stress level, then exposed to saline solutions to observe osmotic consolidation over time.

In the final stage, SEM images were used to examine the microstructure of tested samples. The results revealed that osmotic compression can induce additional settlement beyond that from mechanical loading alone.

The findings confirm that external loads and osmotic stresses must be considered together when assessing soil behavior. Osmotic compression was the dominant mechanism, but changes in fabric and bond formation also contributed to deformation.

2 Material and Method

2.1 Material

To investigate the behavior of natural clays, low- and high-plasticity samples were chosen. From a mineralogical perspective, these samples represent the characteristic behavior of clay soils dominated by smectite and kaolin group minerals. Based on the analysis results, the definition of the components (minerals) in the sample and the estimated proportional composition is shown in Table 1.

Table 1: Mineral definition and estimation for high plasticity(H) and low plasticity(L) sample

	Mineral	Estimated Rate (%)
High Plasticity Sample (CH)	Clay Mineral – Smectite Group	55-60
	Clay Mineral – Kaolinite - Chlorite Group	<5
	Quartz	15-10
	Feldspar	15-20
	Calcite	5-10
Low Plasticity Sample (CL)	Clay Mineral – Smectite Group (Probably irregular) (Probably mixed layer)	Uncertain
	Clay Mineral – Kaolinite - Chlorite Group (Probably mixed layer)	High
	Clay Mineral Illite – Mica Group	Low
	Quartz	15-20
	Feldspar	<5

Atterberg limit tests (liquid limit and plasticity limit) (TS EN ISO 17892-12[40]), specific gravity tests (pycnometer test) (TS EN ISO 17892-3 [41]) and combined granulometry tests (TS EN ISO 17892-4[42]) were performed to determine the index properties of soil samples. The liquid limit is determined by the falling cone method. The test results are summarized in the table below (Table 2).

Table 2: Summary of index parameters

Sample		High Plasticity Sample	Low Plasticity Sample
-No4 (%)		99	99
-No270 (%)		98	98
Specific Gravity		2.70	2.48
Atterberg Limits	**PL**	31	25
	LL	67	46
	PI	36	21
Soil Classification		CH	CL

The samples were prepared by kneading powdered natural clay with distilled water at liquid limit water content. Di Maio [26] demonstrated that the liquid limit of clays decreases sharply with an increase in electrolyte concentration up to 1M, and then decreases more gradually at concentrations above 1M. Based on this observation, saline solutions were selected to reflect the characteristic reduction in liquid limit under increasing electrolyte concentration. To evaluate both the ionic strength and valency effects on clay behavior, NaCl and $CaCl_2$ solutions were prepared at concentrations of 0.1 M, 0.25 M, 1 M, and 2 M.

2.2 Method

2.2.1 Oedometer Test

Following TS EN ISO 17892-12 [43], samples prepared with pure water were subjected to different load levels (12.5, 50, and 200 kPa), and their osmotic consolidation behavior was evaluated by replacing cell water with saline.

Each sample was first saturated with distilled water in the consolidation cell and kept for 24 hours. Loading began the next day at 6.25 kPa and was gradually increased to the target level (12.5, 50, or 200 kPa). The load-deformation behavior was monitored for 1–3 days, depending on plasticity, until secondary compression was achieved. Once this stage was reached, the cell water was drained with a syringe and replaced with saline solution, and the initial water level was marked. To prevent evaporation, the cell was sealed with a flexible PVC sheet cut to fit the cell, with a central opening to allow movement of the loading arm. Despite these precautions, water levels were monitored continuously, and any loss was replenished with distilled water when necessary.

$C\alpha$ is defined as the slope of the linear tail of the deformation-time curve after consolidation [44], [45], [46]. Since no specific standard exists for identifying this linear segment, each author

has proposed their own method based on their approach and the soil's water retention behavior.

Wu et al. [47] preferred to wait at the loading stage until the deformation rate dropped below 0.01 mm/8h. For samples with liquid limits (LL) ranging from 48 to 67, a waiting period of 72 hours (3 days) was applied at each load stage to determine the linear portion of the graph. Deng et al. [48], on the other hand, conducted tests on samples with LL values between 62 and 78, waiting at each load stage until the deformation rate fell to 0.01 mm/h. As these experiments were performed under high loads using specialized oedometer equipment, testing was terminated once the deformation rate stabilized at this threshold. Jiang et al. [49] examined the creep behavior of samples with LL values between 31 and 43, waiting at each load stage until the deformation rate decreased to 0.01 mm/24h, with each load stage lasting 72 hours (3 days). Di Maio et al. [50] utilized clay samples with LL values of 50, 110, and 390. For the LL = 50 (kaolin) sample, the loading process was terminated after 24 hours, whereas for the LL = 390 (bentonite) sample, load stages were extended up to 7 days. In a separate study, Di Maio [26] observed secondary compression in the LL = 390 (bentonite) sample by waiting between 5 and 7 days at each load stage. To investigate osmotic consolidation, a saturated salt solution was introduced, and the settlement rate was monitored for 10 days at each load stage until it stabilized.

Based on the studies outlined above, the recommended waiting periods at each load stage to observe secondary compression are as follows:

LL<30	⇨	24h
30<LL<50	⇨	48h
50<LL<100	⇨	72h - 96h
100<LL<400	⇨	120h -168h

Loading times were determined in a similar manner. For the high-plasticity (CH) samples, each load stage lasted 3 days, while for the low-plasticity (CL) samples, the duration was 1 day. This period continued until the settlement rate of the osmotic-compressed samples matched the secondary compression rate of the samples prepared with distilled water (approximately 0.01 mm/8h or less). As the solution density increased, the duration required to observe its effects extended to as long as 20,000 minutes (14 days).

The experiment was concluded after confirming the completion of osmotic compression at the relevant load level, enabling analysis of fabric changes under load using scanning electron microscopy (SEM). Additionally, further experiments were conducted to study changes in void ratio (e) – logarithm of vertical stress (log p) plots after osmotic compression. For this purpose, the expected loading and unloading stages were performed after osmotic consolidation, marking the end of the experiment.

Reference oedometer tests were performed on salt-treated samples. Loading was applied in seven stages from 6.25 to 400 kPa, followed by unloading in four stages according to the 1/4 rule, in compliance with TS EN ISO 17892-12 [43].

2.2.2 Scanning Electron Microscope (SEM) and Energy Dispersive X-Ray (EDX) Analysis

SEM images were acquired to observe fabric changes in specimens after oedometer tests, focusing on the effects of plasticity, salt molarity and valence, and external loading. The analysis concentrated on changes in tactoids (nm–µm scale clusters) and aggregates (µm-scale clusters). Since no significant changes were observed in platelet structures, high-magnification imaging was not required.

Additionally, energy-dispersive X-ray (EDX) analysis was conducted to determine the cation exchange adsorbed on the clay surfaces. Chemical quantitative analyses of the samples were also performed to supplement the SEM observations.

Energy-dispersive X-ray (EDX) analysis was also conducted to assess cation exchange on the clay surfaces. After oedometer testing, specimens were fractured along the loading axis, and small fragments were extracted. These were coated with gold-palladium (Au-Pd) to enhance image clarity. SEM images were obtained using a Jeol-JSM6510 microscope, and all analyses were carried out at the Central Laboratory of Bingöl University.

3 Results and Discussion

The osmotic compression coefficient provides a reference for comparing settlements due to osmotic effects with those from primary and secondary consolidation. The secondary compression coefficient (Cα) is typically defined as the slope of the linear segment of the deformation-time curve, over one logarithmic cycle after the end of primary consolidation (EOP, t_P) [46], [51]. This definition allows for the derivation of comparable values for the secondary compression coefficient (Cα). As shown in Figure 1, the point where the slope of the osmotic compression curve equals or drops below the secondary compression slope (Cα) indicates the end of the osmotic process. This intersection is used to determine when equilibrium is reached under a given load.

Similar to secondary compression, osmotic compression also continues at a decreasing rate over time. The osmotic compression coefficient ($C\alpha_{osm}$) is defined as the change in void ratio due to osmotic effects divided by the logarithmic change in time: $C_{\alpha_{osm}} = \Delta e_{osm}/\Delta \log t$.

In practice, osmotic compression is considered complete when three consecutive $C\alpha_{osm}$ values are equal to or less than Cα. Figure 1 illustrates the trends of these coefficients and associated time-dependent deformations. The total mechanical compression (Δe_{mech}) is defined as the sum of consolidation (Δe_{cons}) and secondary compression ($\Delta e_{sec.comp}$): $\Delta e_{mech.} = \Delta e_{cons} + \Delta e_{sec.comp.}$.

Changes in pore water concentration affect interparticle forces and the thickness of the diffuse double layer (DDL). Overlapping DDLs act as semi-permeable membranes (allowing the passage of water while restricting the movement of ions), causing a molarity difference between free water and adsorbed water between clay platelets. This difference creates osmotic pressure, which alters the void ratio and leads to settlement known as osmotic compression[25].

During this process, consolidation pressure aids in water removal from platelet surfaces until a new equilibrium is reached between external stress, osmotic forces, and repulsive interactions.

EDX analysis showed that Na^+ and Ca^{2+} concentrations in the clay increased with higher solution molarity and cation valency (Figure 6). This was accompanied by a corresponding increase in osmotic compression (Figure 3), confirming that the effects of ion adsorption and molarity gradients contribute significantly to the microscale consolidation mechanism.

Osmotic compression increases with the molar concentration of the solution in cell for both high- and low-plasticity samples,

thereby contributing more to total settlement. However, its relative share within the overall deformation (mechanical + osmotic) diminishes as the applied load increases (Figure 2). Higher consolidation pressure reduces interplatelet volume rapidly, facilitating faster equilibration between free and adsorbed pore water. The dominant factor in osmotic compression is the thickness of the diffuse double layer (DDL). High-plasticity samples with thicker DDLs exhibit 2% to 38% osmotic compression, whereas low-plasticity samples, having thinner DDLs, show a significantly lower range (0.7%–7.4%). In fact, the osmotic effect is nearly absent in low-plasticity clays due to their limited DDL development.

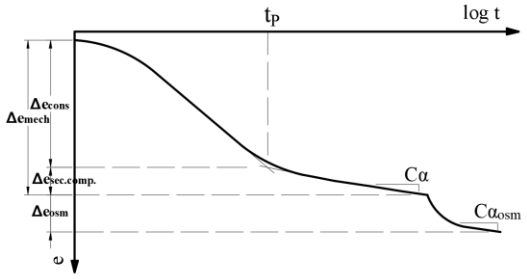

Figure 1: Appearance of time dependent deformation obtained from experiments for osmotic compression.

For both high- and low-plasticity samples, osmotic compression increases with the molar concentration of the added solution, contributing more to total settlement. However, its proportion within the total deformation (mechanical + osmotic) decreases as the applied load increases (Figure 2). This is because higher consolidation pressures reduce interplatelet volume more rapidly, allowing pore water molarity to equilibrate sooner. The key factor controlling osmotic compression is the thickness of the diffuse double layer (DDL): high-plasticity samples, with thicker DDLs, show osmotic compression ranging from 2% to 38%, while low-plasticity samples show a much lower range of 0.7% to 7.4%. In fact, the osmotic effect is nearly absent in low-plasticity samples due to their thin DDLs (Figure 2).

Di Maio [26] examined high-plasticity montmorillonitic clays (LL = 320–400) and showed that exposing pore water to saline solutions could trigger transitional states causing substantial volume changes. At 320 kPa, osmotic compression exceeded mechanical compression, surpassing 100%. Di Maio et al. [8] used bentonite mixtures with varying montmorillonite content and observed approximately 10% osmotic compression even under 40 kPa load when using 0.6M, 1M, and saturated NaCl solutions.

Thyagaraj and Rao [29] conducted studies on the swelling and compression of clays under osmotic effects. In their research, they prepared high plasticity clay (LL = 82) with maximum dry unit weight and worked with 4M NaCl solutions. At a load stage of 200 kPa, they observed approximately 9% osmotic compression. Many similar examples can be found. A common feature of the aforementioned studies is their demonstration that factors such as smectite mineral content, pore water concentration, and dielectric constant are highly decisive in osmotic compression. Alongside the studies summarized above, many other studies have reached similar conclusions. The obtained data are consistent with the findings of previous studies [8], [25], [26], [29], [52].

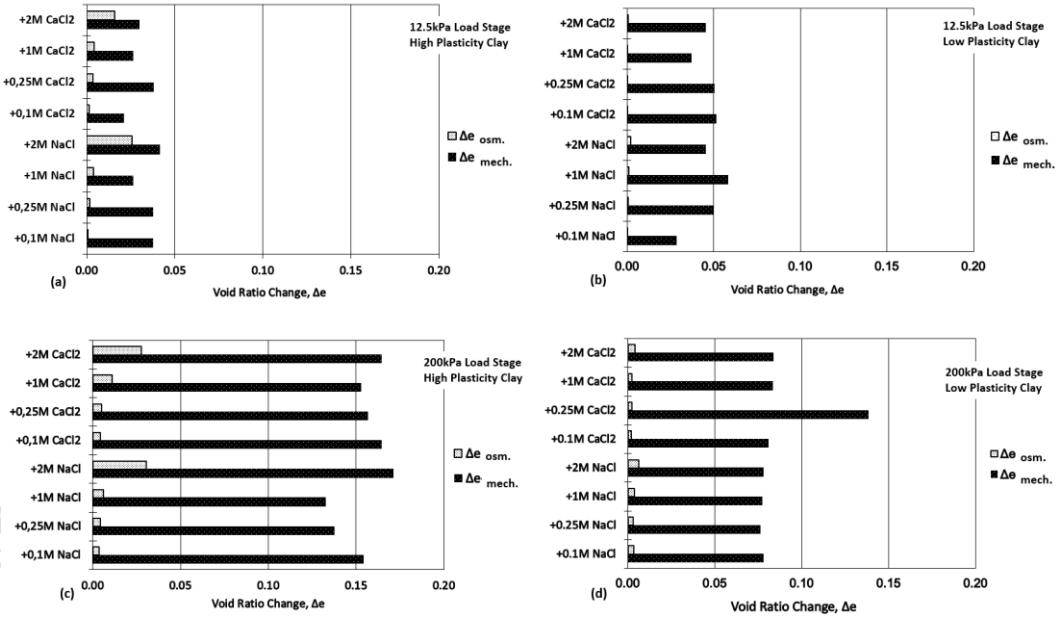

Figure 2: Comparison of mechanical compression and osmotic compression-induced void ratio variation for high plasticity sample for (a)12.5kPa, (b)200kPa load stages; low plasticity sample for (c)12.5kPa, (d)200kPa load stages.

According to Barbour and Fredlund [25], osmotic compression is primarily governed by external load and pore water molarity. The removal of pore water driven by osmotic pressure and facilitated by external load is an integral part of this process.

The most direct evidence of water removal due to osmotic effects is the textural change associated with the collapse of the diffuse double layer (DDL). Di Maio [26] compared SEM images of clay samples exposed to pure water and KCl, showing that the flame-like (evidence of an edge-to-face type fabric) seen in distilled water samples disappeared entirely after salt exposure. This shift toward face-to-face aggregation was attributed to DDL shrinkage. Similar textural transitions were observed in our study with increasing salinity and external loading (Figures 4 and 7).

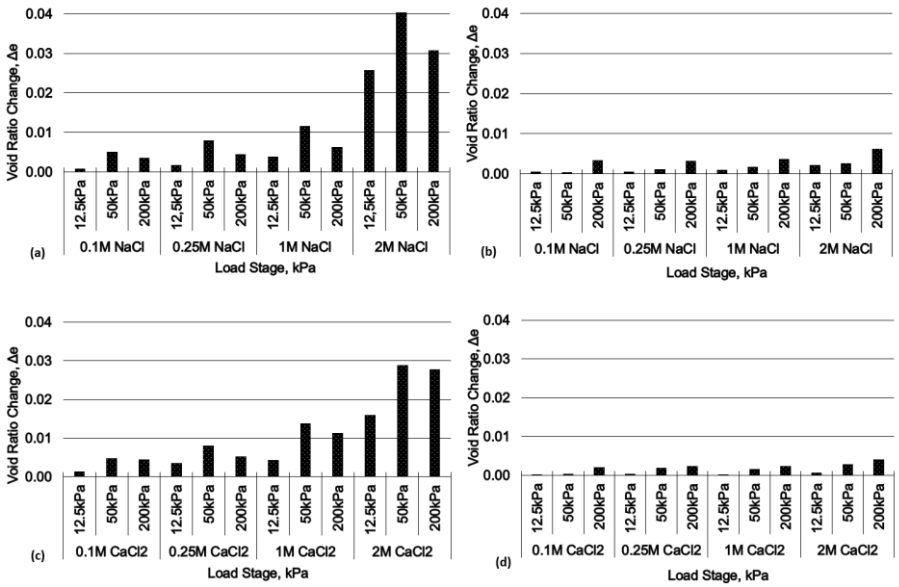

Figure 3: Variation of void ratio with NaCl and $CaCl_2$ solution molarity and consolidation pressure with osmotic effect for high and low plasticity samples [High plasticity samp. (a) NaCl sol. (b) $CaCl_2$ sol.; Low plasticity samp. (c) NaCl sol. (d) $CaCl_2$ sol.]

From this perspective, the osmotic compression of high-plasticity clay, with its greater water adsorption capacity, is expected to exceed that of low-plasticity clay. Similarly, solutions with higher molarity and valence are anticipated to cause greater compression. The data align with these expectations (Figure 3). However, while the highest compression is theoretically expected at 200 kPa consolidation pressure, the maximum compression for high-plasticity clay occurs at 50 kPa (Figure 3), which appears inconsistent with the mechanism proposed by Barbour and Fredlund [25]

Figure 4(a) and (b) show the transformation from flame-like edge-to-face texture to a compact face-to-face structure as stress and molarity increase. For the CL sample, as seen in Figure 5, even 0.1 M $CaCl_2$ at 12.5 kPa is sufficient to eliminate microvoids and induce a sand-like appearance.

Figure 4 shows that in high-plasticity clays treated with NaCl, microvoids decrease with increasing stress, yielding a denser and more homogeneous structure at 200 kPa. At 50 kPa, edge-to-face aggregations (flame-like textures) and localized voids are still visible. Similarly, in $CaCl_2$-treated samples, the texture becomes void-free at 50 kPa, likely due to the rapid DDL collapse induced by divalent cations. These changes illustrate how salt type and load level jointly influence microstructural fabric.

In NaCl-treated samples, flame-like textures persist at 50 kPa but diminish compared to 12.5 kPa. By 200 kPa, the texture shifts to a face-to-face configuration due to mechanical compression, reducing the osmotic effect. At low stress (12.5 kPa), osmotic compression dominates, whereas at 50 kPa, both osmotic and mechanical deformations contribute. These observations highlight the limitations of interpreting osmotic behavior solely through microstructural changes.

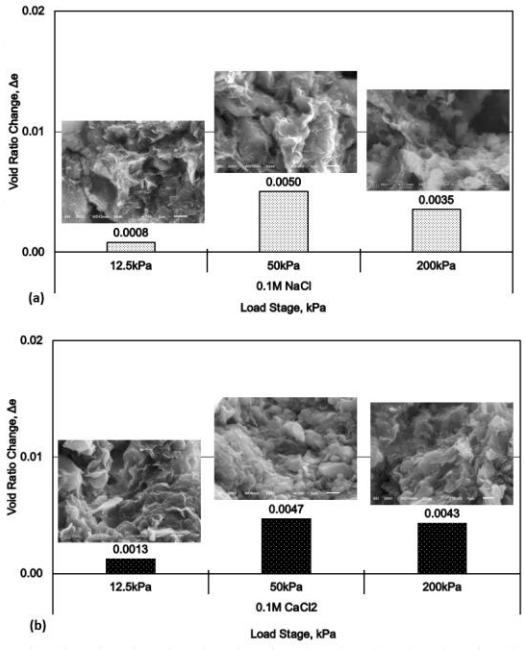

Figure 4: Variation of void ratio and soil fabric with 0.1M solutions and consolidation pressure with osmotic effect for high plasticity sample. [(a) 0.1M NaCl sol.; (b) 0.1M $CaCl_2$ sol.]

The higher compressibility observed at 50 kPa compared to 200 kPa can be attributed to the osmotic mechanism. Under increasing load, equilibrium between free and adsorbed pore water molarities—separated by overlapping DDLs—is achieved more rapidly. At low loads (12.5 kPa), reduced mechanical compression limits this interaction. At 200 kPa, significant reduction in void ratio means less deformation is needed to reach molar balance, resulting in lower osmotic compression.

For the high-plasticity sample prepared with distilled water, the amount of deformation observed at 50 kPa was similar to that recorded at 12.5 kPa and 200 kPa. This suggests that the water volume between platelets—and thus the osmotic response—was at an intermediate level. Although the deformation required to establish equilibrium between the adsorbed and free pore water molarity corresponds to a volume range between 12.5 kPa and 200 kPa, the sample's fabric at 50 kPa still exhibited edge-to-face aggregation. This may explain the higher compressibility and more favorable permeability compared to the 200 kPa sample, indicating a stronger osmotic effect. In contrast, for the CaCl2 solution sample, this mechanism was not observed beyond 50 kPa as it was completed in the 12.5 - 50 kPa load range. The compression due to osmotic consolidation between 50kPa and 200kPa is approximately equal for the same reason (Figure 4b).

Many researchers studying osmotic compression have focused on high-plasticity clays with a high smectite content [25], [26], [29], [52], [53]. Studies conducted on low-plasticity kaolinitic clays are relatively limited; an example is the work by Di Maio et al.[50]. Di maio et al. [50] observed osmotic compression in low-plasticity clays to be negligible. They emphasized that smectite-group clays are one of the critical determinants of osmotic compression behavior. Our observations are consistent with the findings reported by the authors.

In low plasticity samples, the sample texture rapidly changes from edge-to-face type to face-to-face type texture as the sample begins to interact with solutions of low molarity. The textural change that occurs when low plasticity clay samples are exposed to 0.1M NaCl and $CaCl_2$ solutions at 12.5kPa load level can be seen in Figure 5. Due to the salt effect, the more limited flame-like or card pile type appearance in the texture disappears and changes towards a sand-like appearance. This change in appearance indicates that the DDL thickness of the low plasticity clay decreases rapidly and significantly. Therefore, the behavior of the sample exposed to the saline solution can no longer be explained by osmotic principles.

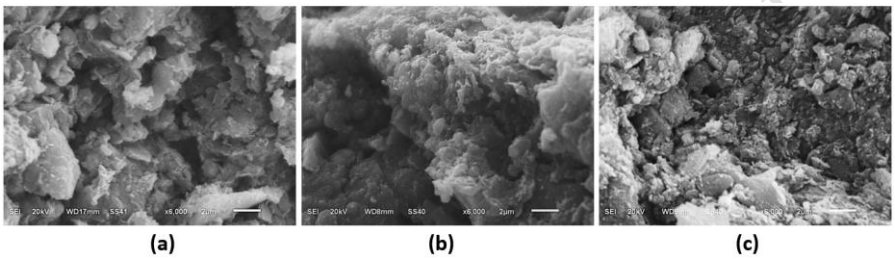

Figure 5: Fabric changes of the low plasticity samples (a) prepared with pure water and (b) 0.1M NaCl solution and (c) 0.1M $CaCl_2$ solution added (12,5kPa load stage)

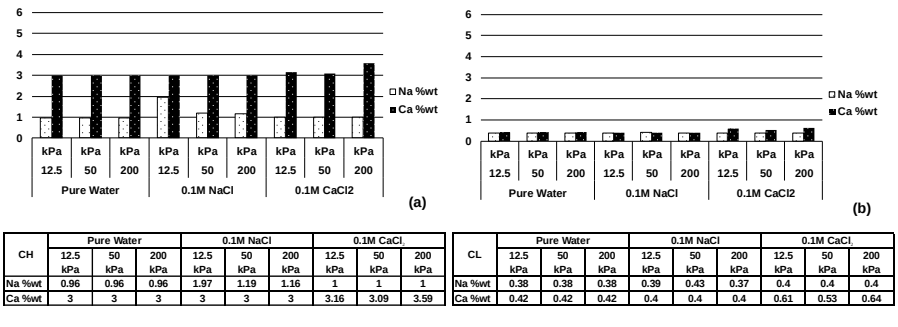

CH	Pure Water			0.1M NaCl			0.1M $CaCl_2$		
	12.5 kPa	50 kPa	200 kPa	12.5 kPa	50 kPa	200 kPa	12.5 kPa	50 kPa	200 kPa
Na %wt	0.96	0.96	0.96	1.97	1.19	1.16	1	1	1
Ca %wt	3	3	3	3	3	3	3.16	3.09	3.59

CL	Pure Water			0.1M NaCl			0.1M $CaCl_2$		
	12.5 kPa	50 kPa	200 kPa	12.5 kPa	50 kPa	200 kPa	12.5 kPa	50 kPa	200 kPa
Na %wt	0.38	0.38	0.38	0.39	0.43	0.37	0.4	0.4	0.4
Ca %wt	0.42	0.42	0.42	0.4	0.4	0.4	0.61	0.53	0.64

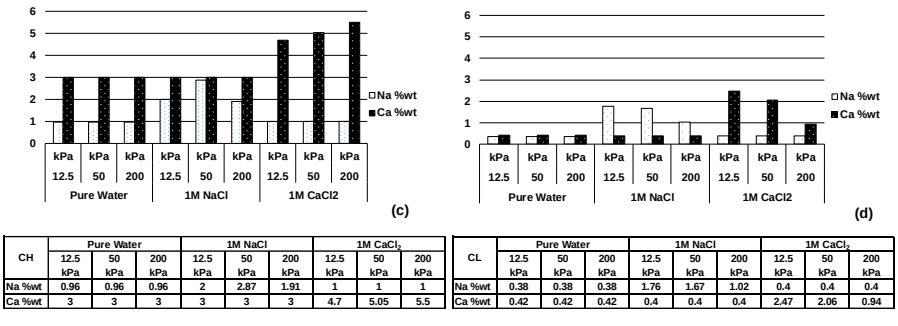

CH	Pure Water			1M NaCl			1M $CaCl_2$		
	12.5 kPa	50 kPa	200 kPa	12.5 kPa	50 kPa	200 kPa	12.5 kPa	50 kPa	200 kPa
Na %wt	0.96	0.96	0.96	2	2.87	1.91	1	1	1
Ca %wt	3	3	3	3	3	3	4.7	5.05	5.5

CL	Pure Water			1M NaCl			1M $CaCl_2$		
	12.5 kPa	50 kPa	200 kPa	12.5 kPa	50 kPa	200 kPa	12.5 kPa	50 kPa	200 kPa
Na %wt	0.38	0.38	0.38	1.76	1.67	1.02	0.4	0.4	0.4
Ca %wt	0.42	0.42	0.42	0.4	0.4	0.4	2.47	2.06	0.94

Figure 6: Variation of % of Na^+ and Ca^{+2} cation in weight (**EDX data**) with NaCl and $CaCl_2$ solution molarity and consolidation pressure with osmotic effect for high and low plasticity samples [(a) High plasticity sample; (b) Low plasticity sample]

As the valency increases, the negatively charged clay surface is expected to achieve charge balance through cation adsorption [37], [45]. As shown in Figure 6, Na+ and Ca+2 percentages increase with molarity. This ionic uptake correlates with the dense textures seen in Figure 7, confirming cation-induced DDL collapse. However, a valence effect could not be observed in the low-plasticity sample due to the reduced thickness of its diffuse double layer. In the high-plasticity sample, the valence effect was observed with slight variations up to a solution density of 1 M. Conversely, the opposite trend was noted for the 2M

solution. This phenomenon can be attributed to the rapid disappearance of micro-pores in the clay fabric of the sample treated with the 1M $CaCl_2$ solution (Figure 7)

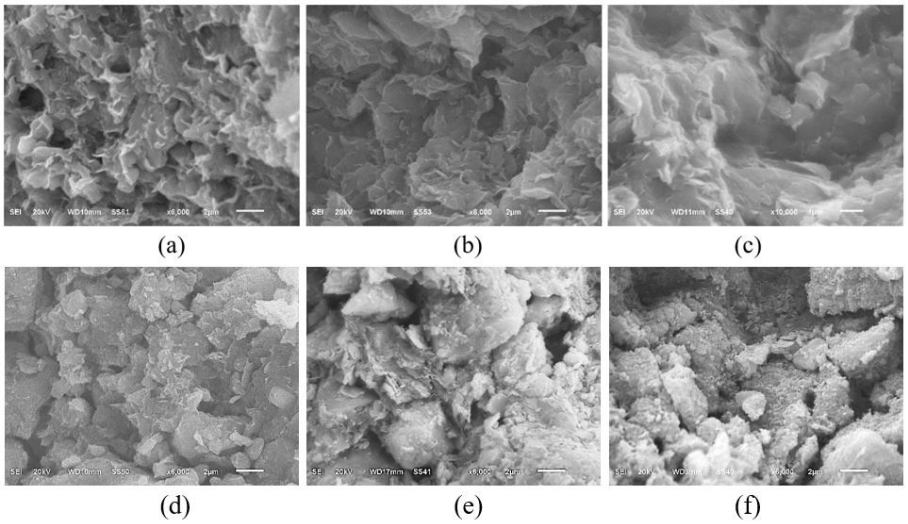

Figure 7: Fabric changes of the high plasticity samples (a) prepared with pure water and (b) 1M NaCl solution and (c) 1M $CaCl_2$ solution added (12,5kPa load stage); low plasticity samples (c) prepared with pure water and (d) 1M NaCl solution and (e) 1M $CaCl_2$ solution added (12,5kPa load stage)

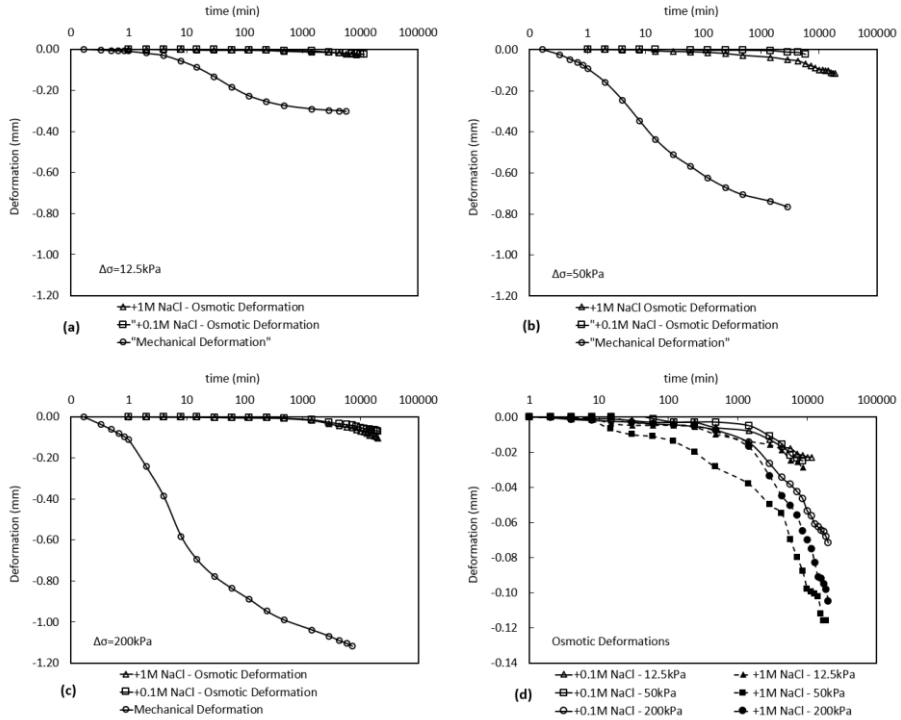

Figure 8: Comparison of the deformation – time graphs of the samples NaCl added high plasticity samples. Osmotic and mechanical deformation comparisons (a)12.5kPa, (b)50kPa, (c) 200kPa and (d)osmotic deformation comparison for all load stages

In saline-treated samples, salt diffuses into the clay from both ends, gradually increasing free pore water molarity. The molarity difference between free and adsorbed water across overlapping DDLs acts like a semi-permeable membrane, triggering outward water migration. This disrupts equilibrium between physicochemical forces, enhancing repulsion. Consolidation pressure facilitates water expulsion, reducing voids and increasing molarity until osmotic and mechanical forces reach balance, leading to settlement.

This process disrupts the equilibrium between physicochemical repulsive and attractive forces, tilting the balance in favor of repulsive forces. The existing external load (consolidation pressure) facilitates the leakage of adsorbed water, reducing the interparticle distance. Consequently, the

volume of adsorbed water decreases while its molar concentration increases. This sequence of events characterizes osmotic settlement. The reduction in void ratio (settlement) ceases when molar concentrations equilibrate, and the compressive forces reach a level sufficient to counteract the applied consolidation pressure, thereby establishing equilibrium between compressive and tensile forces [25].

Although pure water-treated samples exhibit higher compressibility, additional settlement occurs in saline samples due to osmotic compression. As illustrated in Figure 8, the strain of samples prepared using a solution and distilled water at low molar concentrations increases under applied loading; however, the resulting compression magnitudes are notably similar. Conversely, the difference in compression between the samples prepared with pure water and those with a solution closely aligns with the magnitude of osmotic compression.

These findings underline the dominance of osmotic compression in total settlement, with mechanical compression contributing less. Salt exposure, combined with external loading, leads to face-to-face aggregation and reduced compressibility. This structural transition suggests that subsequent e–log p curves may shift upward due to a stiffer post-osmotic fabric.

The void ratio decreases, and the clay fabric undergoes transformation due to the influence of salt, until equilibrium between the repulsive and attractive forces is achieved under consolidation pressure. Under the combined effects of salt and consolidation pressure, face-to-face aggregation becomes more pronounced, resulting in a fabric that is less compressible. The less deformable nature of this new fabric following osmotic compression suggests that subsequent (e;logp) data points are likely to appear above the original e-logp line as loading progresses.

Figure 9 shows a distinct upward shift in the e-logp curve of the sample exposed to saline solution compared to the control. The observed shift in the e-logp relationship for samples transitioning to saline cell water aligns with theoretical expectations. The clay sample, whose structure is altered under the influence of salt, exhibits a new e-logp trajectory as loading continues (Figure 9). Notably, the e-logp curves for clay subjected to osmotic effects differ in orientation and character in subsequent consolidation stages when compared to the initial curve. The resulting consolidation path diverges from the initial trend, as also reported by Barbour [54] and Di Maio [26].

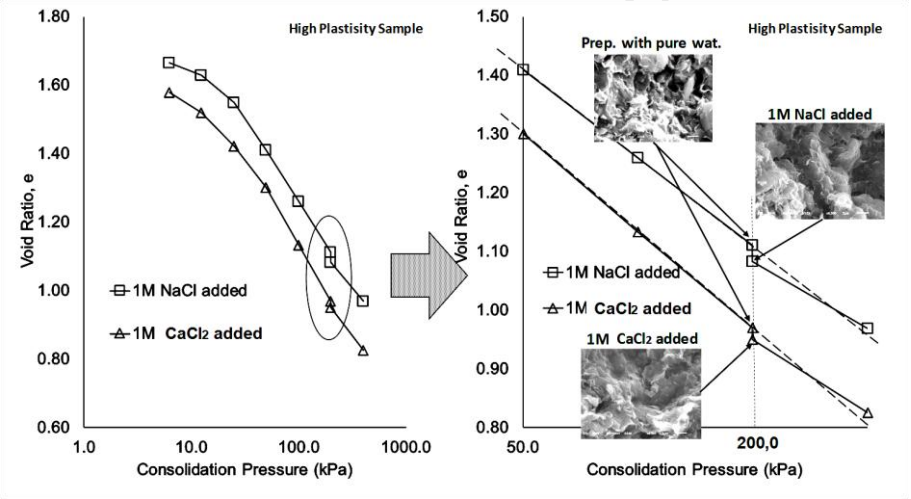

Figure 9: Osmotic effect of leaking salt solutions on void ratio – vertical stress (e-logp) graphs and clay fabric (200kPa load range)

4 Conclusions

Many aspects highlighted in previous studies remain relevant in our research. In osmotic compression, factors such as the clay's smectite mineral content, pore water molarity, and dielectric constant values play a decisive role. Additionally, the balance of external and internal stresses is also identified as a critical determinant for osmotic compression.

The change in void ratio in the osmotic compression process is permanent as long as the internal and external load balances do not change. While the osmotic compression mechanism is a key determinant, it also leads to the formation of new bonds through fabric changes, with mechanical forces contributing to the load transfer mechanism. These additional settlements are considerable when compared to those caused solely by mechanical compression.

Furthermore, the mechanical compression resulting from consolidation pressure during osmotic compression serves a dual role. It reduces the relative contribution of osmotic compression to total compression while simultaneously enhancing the compression induced by the osmotic effect.

In conclusion, the findings underscore the importance of considering external loads in future studies addressing osmotic consolidation to better understand the interplay between these factors.

5 Author contribution statement

This publication was prepared from the PhD thesis titled "……", which was completed at ……. University, Department of Civil Engineering in ……..

Author-1 is the thesis writer, and Author-2 is the thesis advisor. Author contributions to the article writing process were realized in a similar manner.

All data were made available for sharing with the publication of the PhD thesis at the National Thesis Center of the Council of Higher Education Institution. (https://tez.yok.gov.tr/)

6 Ethics committee approval and conflict of interest declaration

There is no need to obtain ethics committee permission for the article prepared.

There is no conflict of interest with any person/institution in the prepared article.

7 References

[1] K. Satake, "Tsunamis," in *Earthquake Seismology*, vol. 4, G. Schubert, Ed., 2007, pp. 483–511. doi: 10.1016/B978-044452748-6.00078-X.

[2] M. A. Baptista and J. M. Miranda, "Revision of the Portuguese catalog of tsunamis," *Natural Hazards and Earth System Sciences*, vol. 9, no. 1, pp. 25–42, 2009, doi: 10.5194/nhess-9-25-2009.

[3] S. Yolsal-Çevikbilen and T. Taymaz, "Earthquake source parameters along the Hellenic subduction zone and numerical simulations of historical tsunamis in the Eastern Mediterranean," *Tectonophysics*, vol. 536–537, pp. 61–100, 2012, doi: https://doi.org/10.1016/j.tecto.2012.02.019.

[4] J. P. Terry, N. Winspear, J. Goff, and P. H. H. Tan, "Past and potential tsunami sources in the South China Sea: A brief synthesis," *Earth Sci Rev*, vol. 167, pp. 47–61, 2017, doi: https://doi.org/10.1016/j.earscirev.2017.02.007.

[5] L. Cordrie, A. Gailler, P. Heinrich, P. Briole, and A. Ganas, "The July 20, 2017 Mw = 6.6 Bodrum-Kos Earthquake, Southeast Aegean Sea: Contribution of the Tsunami Modeling to the Assessment of the Fault Parameters," *Pure Appl Geophys*, vol. 178, no. 12, pp. 4865–4889, 2021, doi: 10.1007/s00024-021-02766-3.

[6] C. Yavuz, K. Yilmaz, and G. Onder, "Combined Hazard Analysis of Flood and Tsunamis on The Western Mediterranean Coast of Turkey," *Natural Hazards and Earth System Sciences Discussions*, vol. 2022, pp. 1–20, Jun. 2022, doi: 10.5194/nhess-2022-121.

[7] NASA, "Sea Surface Salinity From Space - NASA," https://salinity.oceansciences.org/. Accessed: Nov. 16, 2022. [Online]. Available: https://salinity.oceansciences.org/highlights04.htm

[8] C. Di Maio, "Influence of Pore Fluid Composition on Volume Change Behaviour of Clays Exposed to the Same Fluid as the Pore Fluid," in *Chemo-Mechanical Couplings in Porous Media Geomechanics and Biomechanics*, B. Loret and J. M. Huyghe, Eds., Vienna: Springer Vienna, 2004, pp. 1–17. doi: 10.1007/978-3-7091-2778-0_1.

[9] A. Ş. Zaimoğlu, F. Hattatoğlu, and R. K. Akbulut, "Yüke maruz ince daneli zeminlerin donma-çözülme davranışı," *Pamukkale Üniversitesi Mühendislik Bilimleri Dergisi*, vol. 19, no. 3, pp. 117–120, 2013, doi: 10.5505/pajes.2013.35744.

[10] S. Siddiqua, G. Siemens, J. Blatz, A. Man, and B. F. Lim, "Influence of Pore Fluid Chemistry on the Mechanical Properties of Clay-Based Materials," *Geotechnical and Geological Engineering*, vol. 32, no. 4, pp. 1029–1042, 2014, doi: 10.1007/s10706-014-9778-z.

[11] S. Akbulut, Z. N. Kurt, and S. Arasan, "Surfactant modified clays' consistency limits and contact angles," *Earth Sciences Research Journal*, vol. 16, no. 2, pp. 13–19, 2012.

[12] B. K. Dahal and J.-J. Zheng, "Compression behavior of reconstituted clay: A study on black clay," *Journal of Nepal Geological Society*, vol. 55, no. 1, pp. 55–60, 2018, doi: 10.3126/jngs.v55i1.22789.

[13] R. M. Schmitz, C. Schroeder, and R. Charlier, "Chemo–mechanical interactions in clay: a correlation between clay mineralogy and Atterberg limits," *Appl Clay Sci*, vol. 26, no. 1–4, pp. 351–358, Aug. 2004, doi: 10.1016/j.clay.2003.12.015.

[14] H. Bayesteh, M. Sharifi, and A. Haghshenas, "Effect of stone powder on the rheological and mechanical performance of cement-stabilized marine clay/sand," *Constr Build Mater*, vol. 262, p. 120792, Nov. 2020, doi: 10.1016/J.CONBUILDMAT.2020.120792.

[15] H. Bayesteh and A. Bayat, "Volume change behavior of reconstituted marine clay: effect of initial and leaching pore fluid salinity," *Environ Earth Sci*, vol. 80, no. 6, p. 235, 2021, doi: 10.1007/s12665-021-09533-6.

[16] Naeini M. A. and Jahanfar S. A., "Effect of Salt Solution and Plasticity Index on undrain Shear Strength of Clays," *International Journal of Chemical, Molecular, Nuclear, Materials and Metallurgical Engineering*, vol. 5, pp. 92–96, 2011, doi: https://doi.org/10.5281/zenodo.1058403.

[17] Naeini M. A. and Jahanfar S. A., "Effect of Salt Solution and Plasticity Index on undrain Shear Strength of Clays," *International Journal of Chemical, Molecular, Nuclear, Materials and Metallurgical Engineering*, vol. 5, pp. 92–96, Jan. 2011, doi: https://doi.org/10.5281/zenodo.1058403.

[18] K. R. Reddy, P. Yaghoubi, and Y. Yukselen-Aksoy, "Effects of biochar amendment on geotechnical properties of landfill cover soil," *Waste Management & Research*, vol. 33, no. 6, pp. 524–532, 2015, doi: 10.1177/0734242X15580192.

[19] Ö. Çimen, H. İ. Günaydın, and S. N. Keskin, "Effect of construction waste to engineering properties of high Plasticity clay soil," *Pamukkale University Journal of Engineering Sciences*, vol. 23, no. 3, pp. 250–253, 2017, doi: 10.5505/pajes.2016.81567.

[20] M. L. Diallo and Y. S. Ünsever, "An experimental study on the stabilization of a clay soil with construction wastes and lime," *Pamukkale University Journal of Engineering Sciences*, vol. 26, no. 6, pp. 1030–1034, 2020, doi: 10.5505/pajes.2019.51436.

[21] H. I. Inyang, J. L. Daniels, and V. Ogunro, "Engineering controls for risk reduction at Brownfield sites," *American Society of Civil Engineers, Geo-Congress '98*, 1998, doi: https://doi.org/10.1061/9780784403891.016.

[22] C. H. Benson, J. N. Meegoda, R. G. Gilbert, and S. P. Clemence, "Risk-Based Corrective Action and Brownfields Restorations," *American Society of Civil Engineers, Geo-Congress '98*, Oct. 1998, doi: https://doi.org/10.1061/9780784403891.

[23] G. Scaringi and C. Di Maio, "Residual Shear Strength of Clayey Soils: the influence of displacement rate," in *GC Chiorean (ed.), Proc. 2nd Int. PhD Conf. Civ. Eng. & Arch*, 2014, pp. 325–332. Accessed: Nov. 01, 2021. [Online]. Available: https://hdl.handle.net/11563/98898

[24] C. Di Maio and G. Scaringi, "Shear displacements induced by decrease in pore solution concentration on a pre-existing slip surface," *Eng Geol*, vol. 200, pp. 1–9, Jan. 2016, doi: 10.1016/j.enggeo.2015.11.007.

[25] S. L. Barbour and D. G. Fredlund, "Mechanisms of osmotic flow and volume change in clay soils,"

Canadian Geotechnical Journal, vol. 26, no. 4, pp. 551–562, Nov. 1989, doi: 10.1139/t89-068.

[26] C. Di Maio, "Exposure of bentonite to salt solution: Osmotic and mechanical effects," *Geotechnique*, vol. 46, no. 4, pp. 695–707, 1996, doi: 10.1680/geot.1996.46.4.695.

[27] M. Kaczmarek and T. Hueckel, "Chemo-mechanical consolidation of clays: analytical solutions for a linearized one-dimensional problem," *Transp Porous Media*, vol. 32, no. 1, pp. 49–74, 1998, doi: https://doi.org/10.1023/A:1006530405361.

[28] M. Olgun and M. Yıldız, "Effect of organic fluids on the geotechnical behavior of a highly plastic clayey soil," *Appl Clay Sci*, vol. 48, no. 4, pp. 615–621, 2010, doi: https://doi.org/10.1016/j.clay.2010.03.015.

[29] T. Thyagaraj and S. M. Rao, "Osmotic swelling and osmotic consolidation behaviour of compacted expansive clay," *Geotechnical and Geological Engineering*, vol. 31, no. 2, pp. 435–445, 2013, Accessed: Aug. 08, 2021. [Online]. Available: https://link.springer.com/article/10.1007/s10706-012-9596-0

[30] Y. Xu, G. Xiang, H. Jiang, T. Chen, and F. Chu, "Role of osmotic suction in volume change of clays in salt solution," *Appl Clay Sci*, vol. 101, pp. 354–361, 2014, doi: https://doi.org/10.1016/j.clay.2014.09.006.

[31] D. Yang, R. Yan, T. Ma, and C. Wei, "Compressive behavior of kaolinitic clay under chemo-mechanical loadings," *Acta Geotech*, vol. 18, no. 1, pp. 77–94, 2023, doi: 10.1007/s11440-022-01554-0.

[32] G. H. Bolt, "Physico-Chemical Analysis of the Compressibility of Pure Clays," *Géotechnique*, vol. 6, no. 2, pp. 86–93, Jun. 1956, doi: 10.1680/geot.1956.6.2.86.

[33] A. Sridharan, "Engineering behaviour of fine grained soils—a fundamental approach," *Indian Geotechnical Journal: Thirteenth IGS Annual Lecture delivered on the occasion of its 32nd Annual General Session*, pp. 447–540, 1991, Accessed: Mar. 07, 2023. [Online]. Available: https://www.semanticscholar.org/paper/Engineering-Behaviour-of-Fine-Grained-Soils-A-A./014de1727ba69ab3fdaa8f36a55e883de2e21507?utm_source=direct_link

[34] S. M. Rao, A. Sridharan, and S. Chandrakaran, "Consistency Limits Behavior of Bentonites Exposed to Sea-Water," *Marine Georesources & Geotechnology*, vol. 11, no. 3, pp. 213–227, 1993, doi: https://doi.org/10.1080/10641199309379919.

[35] A. Sridharan and Sayamurty P., "Potential-Distance Relationships of Clay-Water Systems Considering the Stern Theory," *Clays Clay Miner*, vol. 44, no. 4, pp. 479–484, 1996, doi: 10.1346/CCMN.1996.0440405.

[36] A. Sridharan and K. Prakash, "Influence of clay mineralogy and pore-medium chemistry on clay sediment formation," *Canadian Geotechnical Journal*, vol. 36, no. 5, pp. 961–966, Nov. 1999, doi: 10.1139/t99-045.

[37] J. K. Mitchell and K. Soga, "Fundamentals of soil Behavior," *John Wiley& Sons, Hoboken, New Jersey, USA*, 2005.

[38] S. M. Rao and T. Thyagaraj, "Swell–compression behaviour of compacted clays under chemical gradients," *Canadian Geotechnical Journal*, vol. 44, no. 5, pp. 520–532, May 2007, doi: 10.1139/t07-002.

[39] T. V. Bharat and A. Sridharan, "Prediction of Compressibility Data for Highly Plastic Clays Using Diffuse Double-Layer Theory," *Clays Clay Miner*, vol. 63, no. 1, pp. 30–42, 2015, doi: 10.1346/CCMN.2015.0630103.

[40] TS EN ISO 17892-12, *Geotechnical investigation and testing - Laboratory testing of soil - Part 12: Determination of liquid and plastic limits*. Ankara: Turkish Standard Institute - TSE, 2018.

[41] TS EN ISO 17892-3, *Geotechnical investigation and testing - Laboratory testing of soil - Part 3: Determination of particle density*. Ankara: Turkish Standards Institute-TSE, 2016.

[42] TS EN ISO 17892-4, *Geotechnical investigation and testing - Laboratory testing of soil - Part 4: Determination of particle size distribution*. Ankara: Turkish Standards Institute-TSE, 2016.

[43] TS EN ISO 17892-5, *Geotechnical investigation and testing - Laboratory testing of soil - Part 5: Incremental loading oedometer test*. Ankara: Turkish Standard Institute - TSE, 2017.

[44] B. M. Das, "Advanced Soil Mechanics (1983)," *Mc-GrawHill, New York*, 1983.

[45] R. D. Holtz, W. D. Kovacs, and T. C. Sheahan, *An Introduction to Geotechnical Engineering. 2nd Edition*, 2nd ed. New Jersey: Pearson, 2010.

[46] T. W. Lambe and R. V. Whitman, *Soil Mechanics*. New York: John Wiley & Sons Inc, 1969. Accessed: Jun. 18, 2022. [Online]. Available: https://www.wiley.com/en-gb/Soil+Mechanics-p-9780471511922

[47] Z. Wu, Y. Deng, Y. Cui, A. Zhou, Q. Feng, and H. Xue, "Experimental Study on Creep Behavior in Oedometer Tests of Reconstituted Soft Clays," *International Journal of Geomechanics*, vol. 19, Mar. 2019, doi: 10.1061/(ASCE)GM.1943-5622.0001357.

[48] Y. F. Deng, Y. J. Cui, A. M. Tang, X. L. Li, and X. Sillen, "An experimental study on the secondary deformation of Boom clay," *Appl Clay Sci*, vol. 59–60, pp. 19–25, 2012, doi: 10.1016/j.clay.2012.02.001.

[49] N. Jiang, C. Wang, Q. Wu, and S. Li, "Influence of structure and liquid limit on the secondary compressibility of soft soils," *J Mar Sci Eng*, vol. 8, no. 9, p. 627, 2020, doi: 10.3390/JMSE8090627.

[50] C. Di Maio, L. Santoli, and P. Schiavone, "Volume change behaviour of clays: The influence of mineral composition, pore fluid composition and stress state," *Mechanics of Materials*, vol. 36, no. 5–6, pp. 435–451, 2004, doi: 10.1016/S0167-6636(03)00070-X.

[51] D. W. Taylor and W. Merchant, "A Theory of Clay Consolidation Accounting for Secondary Compression," *Journal of Mathematics and Physics*, vol. 19, no. 1–4, pp. 167–185, Apr. 1940, doi: 10.1002/sapm1940191167.

[52] S. M. Rao, T. Thyagaraj, and H. R. Thomas, "Swelling of compacted clay under osmotic gradients," *Géotechnique*, vol. 56, no. 10, pp. 707–713, Dec. 2006, doi: 10.1680/geot.2006.56.10.707.

[53] A. J. Staverman, "The theory of measurement of osmotic pressure," *Recueil des Travaux Chimiques des Pays-Bas*, vol. 70, no. 4, pp. 344–352, Jan. 1951, doi: https://doi.org/10.1002/recl.19510700409.

[54] S. L. Barbour, "Osmotic Flow and Volume Change in Clay Soils," Dissertation, University of Saskatchewan, 1986. Accessed: Jun. 15, 2022. [Online]. Available: https://harvest.usask.ca/bitstream/handle/10388/5729/Barbour_Sidney_Lee_1987.pdf?sequence=3&isAllowed=y